Hindawi Publishing Corporation
Journal of Nanomaterials
Volume 2014, Article ID 439873, 10 pages
http://dx.doi.org/10.1155/2014/439873

Research Article

Characterization and *In Vitro* Sustained Release of Silibinin from pH Responsive Carbon Nanotube-Based Drug Delivery System

Julia M. Tan,[1] Govindarajan Karthivashan,[2] Palanisamy Arulselvan,[2] Sharida Fakurazi,[2,3] and Mohd Zobir Hussein[1]

[1] *Materials Synthesis and Characterization Laboratory, Institute of Advanced Technology, Universiti Putra Malaysia (UPM), 43400 Serdang, Selangor, Malaysia*
[2] *Laboratory of Vaccine and Immunotherapeutics, Institute of Bioscience, Universiti Putra Malaysia (UPM), 43400 Serdang, Selangor, Malaysia*
[3] *Department of Human Anatomy, Faculty of Medicine and Health Sciences, Universiti Putra Malaysia (UPM), 43400 Serdang, Selangor, Malaysia*

Correspondence should be addressed to Mohd Zobir Hussein; mzobir@upm.edu.my

Received 21 April 2014; Revised 28 May 2014; Accepted 29 May 2014; Published 23 June 2014

Academic Editor: Naoki Kishi

The objective of the present study was to develop and characterize an *in vitro* sustained release formulation of silibinin (SB) using commercially available carboxylated multiwalled carbon nanotubes (COOH-MWCNTs) and to investigate cytotoxicity action of the synthesized nanohybrid (SB-MWCNTs). The resulting nanohybrid was characterized with Fourier transform infrared (FTIR), Raman spectroscopy, thermogravimetric analysis (TGA), ultraviolet-visible spectrophotometry (UV-Vis), scanning electron microscopy (SEM), and transmission electron microscopy (TEM). FTIR, Raman spectroscopy, and TGA analysis confirmed the adsorption of SB molecules to the COOH-MWCNTs. The release of SB from the COOH-MWCNTs nanocarrier was found to be sustained and pH-dependent. The maximum percentage release of SB from the nanocarrier reached approximately 96.6% and 43.1% within 1000 minutes when exposed to pH 7.4 and pH 4.8 solutions, respectively. It was observed that the release of kinetic behaviour of SB from the MWCNTs nanocarrier conformed well to pseudo-second order kinetic model. The obtained MTT result showed that the SB-MWCNTs exhibited enhanced cytotoxicity to human cancer cell lines in comparison with free SB at lower concentrations. These results suggest that SB-MWCNTs nanohybrid may be a promising nanodrug delivery system with sustained release property for the treatment of cancers.

1. Introduction

There are various definitions currently circulating when it comes to the term nanotechnology. The prefix "nano" is actually originated from the Greek word "nanos" for dwarf and technology refers to the application of science in a particular subject [1]. One nanometer (nm) is equal to one-billionth of a meter and a meter is approximately 39 inches long. According to the declaration made by the United States National Nanotechnology Initiative (NNI), nanotechnology involves research and development at the atomic, molecular, or macromolecular levels at dimensions between 1 and 100 nm to create structures, devices, and systems that are enabled for novel applications.

In recent years, nanobiotechnology (a combination of nanotechnology and biotechnology) especially in medicine, or the so-called nanomedicine, has emerged as one of the most advanced and promising areas. It is extensively used by the academician, particularly in the field of drug delivery. The application of nanotechnology in drug delivery involves the use of carriers and therapeutic agents. Nanoscale drug carriers can significantly enhance the bioavailability and therapeutic efficacy of drugs with reduced side effects. In general, they can be grouped into five categories based on the

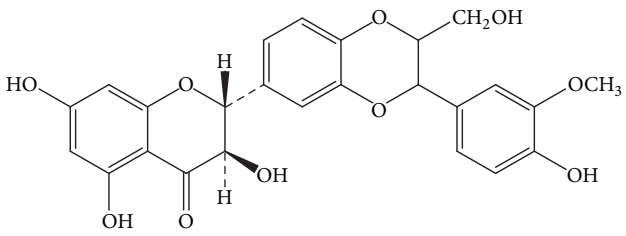

Figure 1: Chemical structure of silibinin.

materials used: polymers, biologics, carbon-based materials, silicon-based materials, or metals [2]. Therapeutic agents are drugs or biologically active materials (e.g., nucleic acids and proteins) which can be entrapped, intercalated, encapsulated, dissolved, adsorbed, or attached onto the drug carriers which can then be tailored for controlled and sustained-release formulations [3–5].

Carbon nanotubes (CNTs) are carbon-based nanoparticles having rolled-up graphene sheets held together by strong interactions of van der Waals to form large aggregates [6]. A single rolled layer of graphite cylinder with a diameter of 0.4 and 2 nm is known as single-walled carbon nanotubes (SWCNTs) [7], whereas multiple concentric cylinders form multiwalled carbon nanotubes (MWCNTs) with a tube diameter ranging from 2 to 100 nm [8]. Both nanotubes have unique electrical, optical, thermal, physical, and chemical properties [9] for the development of advanced nanodrug delivery in therapeutic applications. They possess a very high aspect ratio (L/D of 1 : 1000), allowing multiple loading of various biomolecules to be functionalized on the sidewalls of the CNTs via noncovalent adsorption or covalent conjugation [10]. The chemical modification (functionalization) of CNTs can help to enhance the biocompatibility and solubility for efficient drug delivery because raw CNTs (nonfunctionalized) are water-insoluble and cannot disperse uniformly in aqueous environment. Recent studies have reported that functionalized CNTs can passively cross cell membranes and deliver attached drugs or bioactives through the enhanced permeability and retention effect without causing any harm to the targeted cells [11, 12].

There has been significant progress in the research of functionalized CNTs for the advanced delivery of drugs and biomolecules in biology and nanomedicine [13]. A multitude of strategies have been exploited to deliver anticancer drugs (e.g., topoisomerase inhibitors, antimicrotubules antimetabolites, and platinum-based drugs), non-anticancer drugs (e.g., anti-inflammatories, antioxidants, antimicrobials, and antihypertensives), and biomolecules such as antibodies [14], small interference ribonucleic acids (siRNA) [15], and peptide-based vaccines [16] for controlled and targeted drug delivery. Therefore, the emerging field of CNT-mediated drug delivery system no doubt can be expected to generate promising outcomes for delivery of a variety of therapeutic agents.

Silibinin (Figure 1), also known as silybin, is the major polyphenolic flavonoid extracted from the milk thistle *Silybum marianum* and has been used traditionally as a liver-protective remedy for over 2000 years. Silibinin (SB) can be considered as a safe dietary supplement because it exhibits very low toxicity [17] in humans and animals, possibly due to its antioxidant property [18]. In recent years, studies have suggested that SB possess antiproliferative and anticarcinogenic effects in various cancer cell lines, including skin, colon, prostate, ovarian, and bladder cancers [19–21]. This implicates that SB is a potential drug to treat illnesses related to different types of cancer. However, its effectiveness has been extremely restricted due to its poor aqueous solubility [22] and resulting in poor oral bioavailability, that is, 23–47% [23], after administration. Thus, large dose of SB is required to achieve therapeutic plasma levels. In meeting this demand, a variety of delivery systems have been developed by researches around the globe in order to improve its solubility and thereby bioavailability. For example, formulations using stealth solid lipid nanoparticles [24], mixed micelles [25], microemulsion [26], nanosuspensions [27], porous silica nanoparticles [28], liposomes [23], and nano/microhydrogel matrices [29] as drug carriers have been extensively employed for the enhancement of bioavailability of the poorly water-soluble drug SB.

The present study therefore aimed at developing a simple strategy for the conjugation between SB and MWCNTs, secondly, investigating the drug release profile of SB from the CNT-mediated drug delivery system, and thirdly, assessing the cytotoxicity characteristics of MWCNTs functionalized with SB towards human cancer cells (HepG2 and A549).

Table 1: The properties of the commercial multiwalled carbon nanotubes provided by the manufacturer.

Properties	Short carboxyl multiwalled carbon nanotubes (COOH-MWCNTs)
Outside diameter (nm)	20–30
Length (μm)	0.5–2.0
COOH content (wt.%)	1-2
Purity (wt.%)	>95
Ash (wt.%)	<1.5

2. Materials and Methods

Commercially available multiwalled carbon nanotubes (MWCNTs) were purchased from Chengdu Organic Chemicals Co., Ltd., Chinese Academy of Sciences (Chengdu, China). They consist of short carboxyl carbon nanotubes, where some –COOH groups have been grafted onto the surface of CNTs. Detailed information for the purchased CNTs is included in Table 1. The commercial silibinin (>98% pure as checked by HPLC analysis) was purchased from Sigma-Aldrich (Buchs, Switzerland). HepG2 (human liver hepatocellular carcinoma cell line), and A549 (human lung adenocarcinoma epithelial cell line) were purchased from ATCC (USA). All the other chemicals and solvents were of analytical grade. Purified water was produced by a Millipore water purification system.

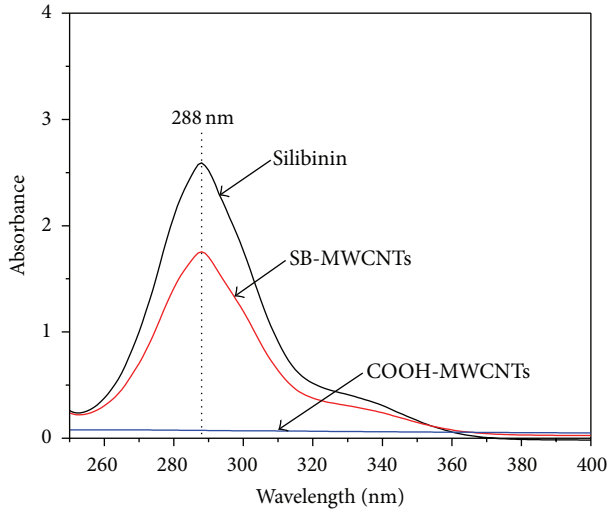

Figure 2: UV-Vis absorption spectra of silibinin, SB-MWCNTS, and COOH-MWCNTs.

2.1. Conjugation of MWCNTs with SB. SB was conjugated to the COOH-MWCNTs by a simple method without using any cross-linker agent. 10 mg of COOH-MWCNTs was dispersed in a 5 mL of ethanol followed by sonication in a water bath for 1 h at room temperature and later added to SB solution (2 mg of SB fully dissolved in 40 mL of 99.8% ethanol). The mixture was then stirred continuously using magnetic stirrer for 20 h at room temperature in darkness. This is to prevent degradation of the drug. Subsequently, the final product (SB-MWCNTs) was collected by filtration, repeated centrifugation, and washing with deionized water to remove excessive SB. Finally, the sample was dried in an oven at 60°C overnight. To determine the amount of unbound SB, the absorbance of the centrifuged solution and free SB were measured at wavelength of 288 nm, which is the characteristic absorbance of SB (Figure 2).

2.2. Physicochemical Characterization of SB-MWCNTs. The drug loading capacity and controlled-release profiles of the nanohybrid were determined by a Lambda 35, ultraviolet-visible spectrophotometer (Perkin Elmer) at a wavelength of 288 nm. The drug loading capacity was calculated using the following formula:

$$\text{Drug loading} = \frac{\text{weight of (initial drug} - \text{unbound drug)}}{\text{weight of initial drug}} \times 100\%. \quad (1)$$

The drug loading capacity was estimated to be ~ 35.1%.

The formation of SB-MWCNTs nanohybrid was confirmed by studying the characteristic absorption bands associated with functional groups of –COOH and SB molecules using Fourier transform infrared (FTIR) spectroscopy. The samples were recorded at wavelengths ranging from 500 to 4000 cm^{-1} on a Thermo Nicolet Nexus FTIR spectrophotometer (model Smart Orbit). For FTIR measurement, the samples were prepared and mixed with potassium bromide (KBr) powder and formed into pellets. Raman spectroscopy measurements were performed on powdered samples using a RamanMicro 200 (Perkin Elmer) instrument at an excitation wavelength of 785 nm. Thermogravimetric studies were performed on a TGA Q500 (TA instruments) to determine the actual drug loading. The samples were heated from 25 to 1000°C with a heating rate of 10°C/min under a nitrogen purge of 40 mL/min.

The surface morphology of the sample was analyzed via scanning electron microscope (SEM). The sample was placed on a stub and sputter coated with gold and examined at 5 kV in a JEOL JSM-7600F field emission scanning electron microscope. Transmission electron microscope (TEM) micrographs were obtained using a Hitachi H-7100 by placing a droplet of sonicated dispersion of the sample directly on the carbon-coated copper grid and dried at 37°C for 24 h.

2.3. In Vitro Drug Release Studies. The drug release experiment from SB-MWCNTs was studied on different human body simulated pH 7.4 and 4.8 phosphate-buffered saline (PBS) solutions. About 11.43 mg of the nanohybrid sample was added to 40 mL of the PBS solutions. The amount of SB released in the solution was measured at predetermined time intervals using a UV-Vis spectrophotometer at 288 nm.

2.4. Cell Lines and Culture Conditions. HepG2 and A549 cell lines were cultured in RPMI 1640 medium supplemented with 10% fetal bovine serum (FBS) and 1% penicillin/streptomycin and cultivated as adherent monolayers in T75 flasks at 37°C in a humidified atmosphere of 5% CO_2. Cells were subcultured (i.e., at approximately 80% confluence) using 0.25% trypsin-EDTA solution for all the experiments.

2.5. Determination of Cytotoxicity (MTT Assay). For the MTT [3-(4,5-dimethylthiazol-2-yl)-2,5-diphenyltetrazolium bromide] assay, all cancer cells were seeded at a density of 1×10^4 cells per well in 100 μL of culture medium in 96-well plates and incubated at 37°C in a 5% CO_2 atmosphere for 24 hours before being used in cell viability assays. The SB compound, COOH-MWCNTs, and nanohybrid were prepared at various concentrations, and the treated cells were incubated for 72 hours. Subsequently, 20 μL of freshly prepared MTT solution was added to each well and culture plates were incubated at 37°C for 3 hours until a purple-colored formazan product developed. The solution in each well, containing media, unbound MTT, and dead cells, was removed and 100 μL of dimethyl sulfoxide (DMSO) was added to each well and the solution was vigorously mixed to dissolve the reacted dye. The absorbance of each well was read on a microplate reader at a test wavelength of 570 nm. All assays were done with three parallel samples in triplicate independently. The cytotoxicity of the free drug, COOH-MWCNTs, and nanohybrid were expressed as the percentage of cell viability with respect to control cells.

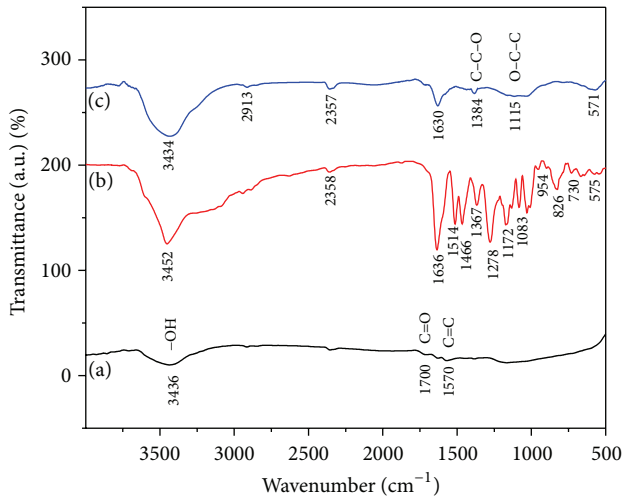

Figure 3: FTIR spectra of (a) COOH-MWCNTs, (b) silibinin, and (c) SB-MWCNTs nanohybrid.

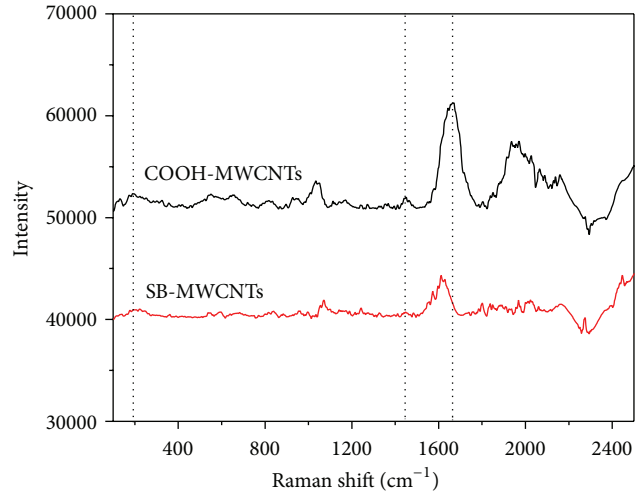

Figure 4: Raman spectra of COOH-MWCNTs and SB-MWCNTs nanohybrid.

2.6. Statistical Analysis. Statistical analysis was performed using the statistical package for social science (SPSS) version 20.0. Results were analysed by one-way analysis of variance (ANOVA). Data were expressed as mean ± standard deviation (mean ± SD). A difference was considered to be significant at $P < 0.05$.

3. Results and Discussions

3.1. Fourier Transform Infrared Spectroscopy. To determine the presence of reactive groups on the COOH-MWCNTs surface after conjugation of SB molecules, Fourier transform infrared spectroscopy (FTIR) was used. The FTIR spectra of commercially purchased COOH-MWCNTs, SB, and SB-MWCNTs nanohybrid are shown in Figure 3. The peak at 3436 and 1700 cm^{-1} (Figure 3(a)) is associated with the presence of hydroxyl group (–OH) and the C=O stretching of the carboxylic acid group (–COOH), respectively. Similar FTIR observation was also reported by a group of researchers for their work on the synthesis of carboxylated MWCNTs [30]. Another peak at around 1570 cm^{-1} of the nanotubes corresponds to C=C stretching vibration in the carbon skeleton [31]. Figure 3(b) shows the spectrum of the pure SB where the characteristic absorption due to the –OH stretching vibration occurs at 3452 cm^{-1} [32]. When the COOH-MWCNTs and drug interact, the FTIR spectra will show broadening of the functional groups and band shift compared to that of the nanocarrier and pure drug. As presented in Figure 3(c), the absorption band was slightly shifted from 1636 cm^{-1} for the C=O stretching in pure SB to 1630 cm^{-1} in nanohybrid. Each –COOH moiety of the nanocarrier has C=O and –OH groups that can potentially form hydrogen bonds with SB [33].

3.2. Raman Scattering Studies. Raman spectroscopy is a powerful technique widely used to characterize the structural quality of functionalized CNTs. As shown in Figure 4, the G- and D-bands of COOH-MWCNTs were exhibited at

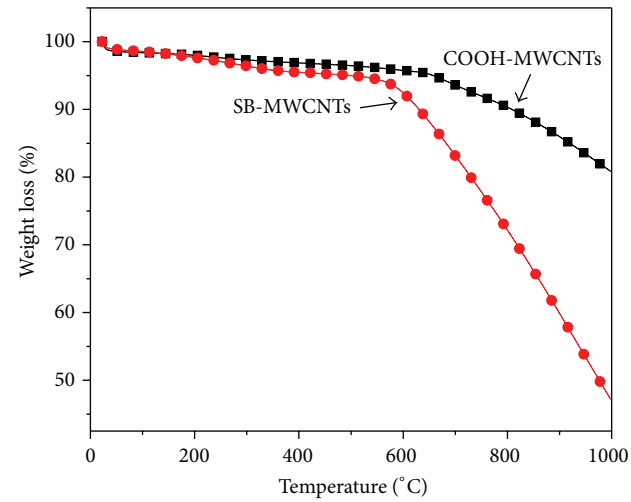

Figure 5: TGA thermograms of COOH-MWCNTs nanocarrier and SB-MWCNTs nanohybrid in nitrogen atmosphere.

1665 cm^{-1} and 1447 cm^{-1} which were assigned to the in-plane E_2g zone-center mode and disorder-induced mode, respectively. The Raman spectrum of the SB-MWCNTs nanohybrid does not show recognizable D-band and the G-band peak intensity was much weaker and slightly shifted towards lower frequency compared to that of the COOH-MWCNTs. This indicates that the characteristic absorption peaks were strongly attenuated due to the conjugation process [34], hence confirming that the interactions between COOH-MWCNTs and drug are strong enough to change the structural pattern of the nanotubes [35]. Furthermore, the radial breathing modes are too weak to be detected due to the large diameters of the nanotubes used in this study.

3.3. Thermogravimetric Analysis. TGA thermograms of COOH-MWCNTs and SB-MWCNTs nanohybrid are demonstrated in Figure 5. The TGA result shows that the

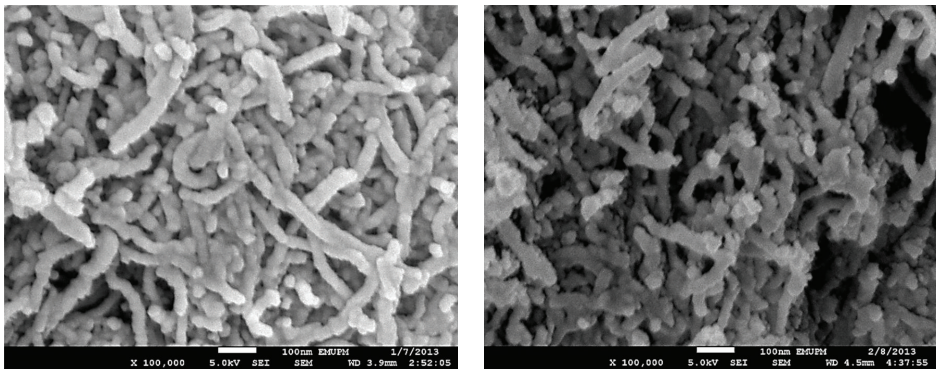

(a) (b)

Figure 6: FESEM images of (a) COOH-MWCNTs and (b) SB-MWCNTs nanohybrid.

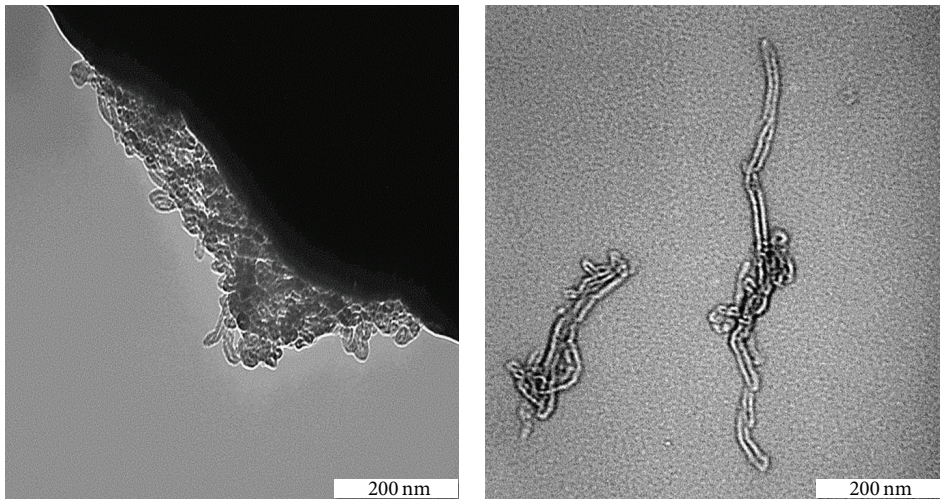

(a) (b)

Figure 7: Low resolution TEM images of (a) COOH-MWCNTs sample and (b) synthesized SB-MWCNTs nanohybrid.

weight loss from the nanocarrier in the temperature range of 125–750°C is approximately 6.4%, which is the typical weight loss for acid-functionalized MWCNTs [34]. The weight loss occurred in the 125°C to 425°C region may be attributed to the evaporation of absorbed water as well as decomposition of carboxyl functionalities attached to the MWCNTs walls [36–38]. Subsequently, the weight loss in the temperature range between 425°C and 625°C corresponds to the removal of hydroxyl groups from the surface of nanotubes [39]. Finally, the residue at 625°C and above should be explained by the oxidation of the remaining disordered carbon in the sample [40]. In the heating up to 1000°C, both COOH-MWCNTs and SB-MWCNTs lost about 19.1% and 52.8% of total weight, respectively. Therefore, approximately 34 wt% of the mass loss was due to the decomposition of SB, further confirming that SB molecules have been adsorbed to COOH-MWCNTs. This finding is in agreement with the drug loading capacity determined by ultraviolet-visible spectrophotometer where the percentage of drug loading was calculated to be around 35.1%.

3.4. Surface Morphology. The microstructures of the COOH-MWCNTs as well as the synthesized SB-MWCNTs nanohybrid were studied by FESEM and TEM. Figure 6 presents FESEM images of MWCNTs before (Figure 6(a)) and after drug conjugation (Figure 6(b)). As seen in Figure 6(a), the nanotubes have a short, tubular topology with smooth surface and they are held together into bundles [30] while Figure 6(b) demonstrates the rougher surface of the MWCNTs and they appear to be in a slightly dispersed form. Similar observation has been reported in the literature for related drug-MWCNTs experiment [41]. Figure 7(a) illustrates the typical TEM image of COOH-MWCNTs in which the nanotubes are seen bundled together as observed in FESEM (Figure 6(a)) and Figure 7(b) shows more exfoliated nanotubes after drug conjugation.

3.5. In Vitro Drug Release Study. The cumulative release profile of SB from MWCNTs in PBS solutions is presented in Figure 8. The amount of SB released from the MWCNTs

Table 2: Correlation coefficient (R^2) and rate constants (k) obtained by fitting the silibinin release data for the COOH-MWCNTs in phosphate-buffered saline solutions at pH 7.4 and pH 4.8.

pH	Saturation release (%)	R^2			k^* (mg/min)
		Pseudo-first order	Pseudo-second order	Parabolic diffusion	
7.4	96.6	0.9488	0.9980	0.7872	1.82×10^{-4}
4.8	43.1	0.7927	0.9955	0.8392	4.13×10^{-4}

*Estimated using pseudo-second order kinetics.

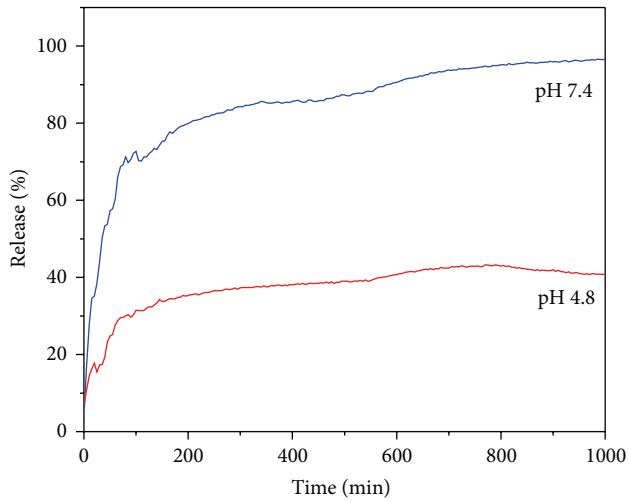

Figure 8: Release profiles of silibinin from MWCNTs at pH 7.4 and pH 4.8 up to 1000 minutes.

was very rapid at the first 100 minutes when exposed to pH 7.4 and pH 4.8 solutions, respectively. Subsequently, the release of SB became much slower and sustained, with total release equilibrium of approximately 96.6% within 1000 minutes at pH 7.4 and 43.1% within 800 minutes at pH 4.8. This process may be attributed to the different extents of COOH ionizations in aqueous solution of different pH values, indicating that the release rate of SB from the nanocarrier is pH-dependent. It was also observed that the SB-MWCNTs nanohybrid has a higher release profile when exposed to pH 7.4 compared to pH 4.8. This is because the higher the pH values, the more carboxylate anions would be produced to form homogenous solution [42], giving rise to a higher solubility of the nanocarrier.

To determine the release kinetics of SB from the nanocarrier, three kinetic models, namely, pseudo-first order equation (2), pseudo-second order equation (3), and parabolic diffusion equation (4), were used [43–45]:

$$\ln(q_e - q_t) = \ln q_e - k_1 t, \quad (2)$$

$$\frac{t}{q_t} = \frac{1}{k_2 q_e^2} + \frac{t}{q_e}, \quad (3)$$

$$\frac{(1 - M_t/M_0)}{t} = kt^{-0.5} + b, \quad (4)$$

where q_e and q_t refer to the equilibrium release amounts at time t, k is a constant corresponding to release amount, and M_0 and M_t represent the drug content remaining in SB-MWCNTs at release time 0 and t, respectively, and b is a constant.

By fitting the control release data of SB from MWCNTs nanocarrier using the above kinetic models, it was observed that the pseudo-second order kinetic model was best to describe the release kinetic behaviour of SB from the MWCNTs nanocarrier. Figure 9 presents the plot of the fitting of SB released from MWCNTs nanocarrier and the corresponding correlation coefficient (R^2) and k values are shown in Table 2. At pH 7.4, both R^2 and k values are 0.9980 and 1.82×10^{-4} mg/min, respectively, and at pH 4.8, the corresponding values are 0.9955 and 4.13×10^{-4} mg/min, respectively.

3.6. In Vitro Anticancer Effect of SB-MWCNTs. In order to evaluate the potential application of the synthesized nanohybrid in nanomedicine and to understand their cytotoxicity nature, *in vitro* cytotoxicity tests were conducted on two human cancer cell lines (HepG2 cells and A549 cells). The treatment time was 72 h. The cell viability was examined by MTT assay (Figure 10) at different gradient concentrations of 0.78, 1.56, 3.13, 6.25, 12.50, 25, and 50 μg/mL.

Since SB has demonstrated its carcinogenic potential for the treatment of cancer [46, 47], we hereby investigated the response of two human cancer cell lines, that is, HepG2 (human liver cancer cells) and A549 (human lung cancer cells). Based on the results presented in Figures 10(a) and 10(b), SB-MWCNTs nanohybrid significantly inhibited proliferation of cancer cells especially A549 cells, at lower concentrations of 1.56–6.25 μg/mL when compared to free drug alone. Although the same concentrations of SB-MWCNTs and free drug are compared, the amount of drug loaded onto MWCNTs (34% wt as determined by TGA analysis) is actually much lower than the amount of free drug used in the assay. Therefore, this sustained release formulation can be used to enhance the efficiency of cancer therapy with reduced drug-related side effects. In addition, further cellular and molecular investigations will be necessary to examine its cytotoxic nature in drug delivery and controlled release applications.

4. Conclusions

The SB molecules were conjugated to MWCNTs by a simple method based on commercially available carboxylated MWCNTs. The chemical conjugation between COOH-MWCNTs and SB molecules has been confirmed by FTIR spectroscopy, Raman, and TGA studies. The FTIR results

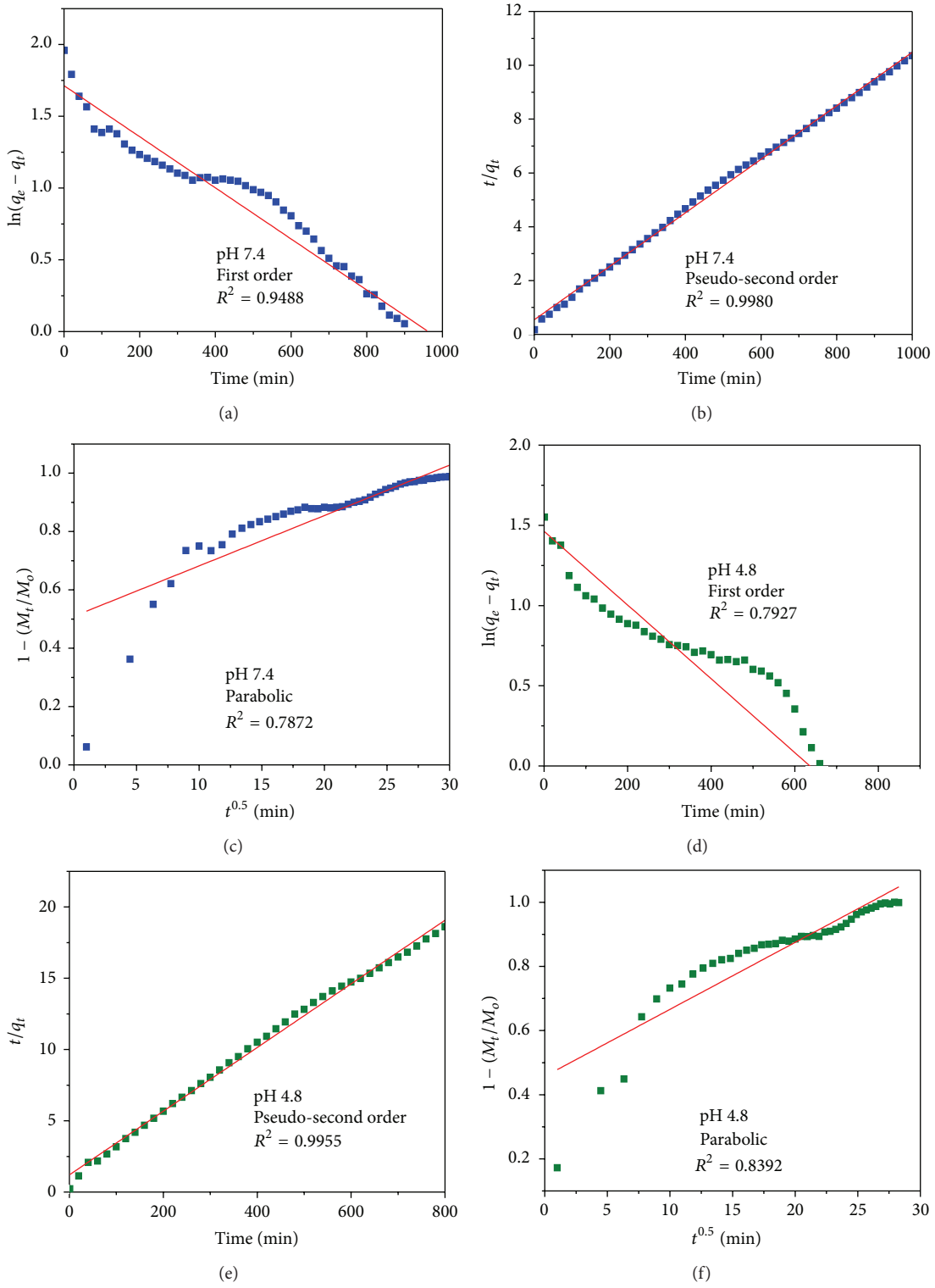

Figure 9: Fitting data of SB from MWCNTs nanocarrier into PBS solutions at pH 7.4 and pH 4.8 using pseudo-first and pseudo-second order kinetics and parabolic diffusion model. The release of kinetic behaviour of SB from its nanocarrier conformed well to pseudo-second order.

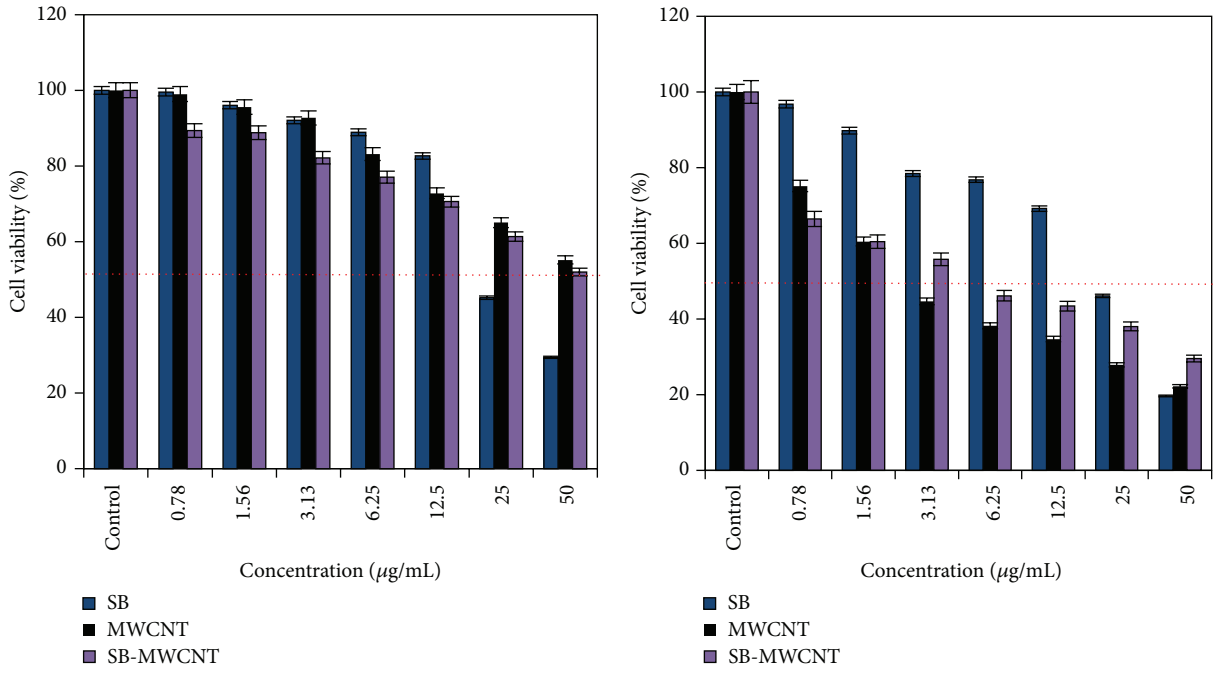

Figure 10: Effect of silibinin (SB), multiwalled carbon nanotubes (MWCNTs), and nanohybrid (SB-MWCNT) on cell viability of human cancer cells (a) HepG2 cells and (b) A549 cells for 72 h of treatment at various concentrations. Cell viability was measured by the MTT method as described in Materials and Methods. Data are shown as means ± SD values obtained from three separate experiments. A difference was considered to be significant at $P < 0.05$.

show the presence of carboxylic (at 1630 cm^{-1} C=O) and ester groups (at 1384 cm^{-1} C–C–O and 1115 cm^{-1} O–C–C) in the SB-MWCNTs nanohybrid. The attachment of SB molecules to COOH-MWCNTs is confirmed by the shift of the C–C–O and O–C–C stretching peak in the SB-MWCNTs sample. Raman spectroscopy and TGA analysis provided further support for the success of chemical conjugation between nanocarrier and drug. Release of the drug from the nanocarrier was observed to occur in a sustained- and pH-dependent manner, suggesting that this nanohybrid could be developed as a sustained- and controlled-release formulation for SB. It was observed that the release kinetic behaviour of SB from the MWCNTs nanocarrier conformed well to pseudo-second order.Proliferation assay against cancer cells indicates that SB-MWCNTs expressed cytotoxicity at lower dosages in comparison with free drug. These preliminary results justify further development of this formulation for drug delivery in nanomedicine.

Conflict of Interests

The authors report no conflict of interests in this work.

Acknowledgments

This work was supported by the Ministry of Science, Technology and Innovation of Malaysia (MOSTI) under National Nanotechnology Directorate, Grant no. NND/NA/(1)/TD11-010 (UPM Vot no. 5489100). Julia M. Tan is grateful to MyBrain15 program for MyPhD scholarship.

References

[1] C. Buzea, I. I. P. Blandino, and K. Robbie, "Nanomaterials and nanoparticles: sources and toxicity," *Biointerphases*, vol. 2, no. 4, pp. MR17–MR172, 2007.

[2] G. A. Hughes, "Nanostructure-mediated drug delivery," *Nanomedicine: Nanotechnology, Biology, and Medicine*, vol. 1, no. 1, pp. 22–30, 2005.

[3] D. Dorniani, A. U. Kura, S. H. Hussein-Al-Ali et al., "*In vitro* sustained release study of gallic acid coated with magnetite-PEG and magnetite-PVA for drug delivery system," *The Scientific World Journal*, vol. 2014, Article ID 416354, 11 pages, 2014.

[4] F. Barahuie, M. Z. Hussein, S. H. Hussein-Al-Ali, P. Arulselvan, S. Fakurazi, and Z. Zainal, "Preparation and controlled-release studies of a protocatechuic acid-magnesium/aluminumlayered double hydroxide nanocomposite," *International Journal of Nanomedicine*, vol. 8, pp. 1975–1987, 2013.

[5] X. Luo, C. Matranga, S. Tan, N. Alba, and X. T. Cui, "Carbon nanotube nanoreservior for controlled release of anti-inflammatory dexamethasone," *Biomaterials*, vol. 32, no. 26, pp. 6316–6323, 2011.

[6] J. E. N. Dolatabadi, Y. Omidi, and D. Losic, "Carbon nanotubes as an advanced drug and gene delivery nanosystem," *Current Nanoscience*, vol. 7, no. 3, pp. 297–314, 2011.

[7] S. Iijima, "Carbon nanotubes: past, present, and future," *Physica B: Condensed Matter*, vol. 323, no. 1–4, pp. 1–5, 2002.

[8] S. Peretz and O. Regev, "Carbon nanotubes as nanocarriers in medicine," *Current Opinion in Colloid and Interface Science*, vol. 17, no. 6, pp. 360–368, 2012.

[9] F. Lu, L. Gu, M. J. Meziani et al., "Advances in bioapplications of carbon nanotubes," *Advanced Materials*, vol. 21, no. 2, pp. 139–152, 2009.

[10] K. Kostarelos, L. Lacerda, G. Pastorin et al., "Cellular uptake of functionalized carbon nanotubes is independent of functional group and cell type," *Nature Nanotechnology*, vol. 2, no. 2, pp. 108–113, 2007.

[11] A. A. Bhirde, V. Patel, J. Gavard et al., "Targeted killing of cancer cells in vivo and in vitro with EGF-directed carbon nanotube-based drug delivery," *ACS Nano*, vol. 3, no. 2, pp. 307–316, 2009.

[12] Z. Liu, K. Chen, C. Davis et al., "Drug delivery with carbon nanotubes for *in vivo* cancer treatment," *Cancer Research*, vol. 68, no. 16, pp. 6652–6660, 2008.

[13] B. S. Wong, S. L. Yoong, A. Jagusiak et al., "Carbon nanotubes for delivery of small molecule drugs," *Advanced Drug Delivery Reviews*, vol. 65, no. 15, pp. 1964–2015, 2013.

[14] M. R. McDevitt, D. Chattopadhyay, B. J. Kappel et al., "Tumor targeting with antibody-functionalized, radiolabeled carbon nanotubes," *Journal of Nuclear Medicine*, vol. 48, no. 7, pp. 1180–1189, 2007.

[15] J. E. Podesta, K. T. Al-Jamal, M. A. Herrero et al., "Antitumor activity and prolonged survival by carbon-nanotube-mediated therapeutic sirna silencing in a human lung xenograft model," *Small*, vol. 5, no. 10, pp. 1176–1185, 2009.

[16] D. Pantarotto, C. D. Partidos, J. Hoebeke et al., "Immunization with peptide-functionalized carbon nanotubes enhances virus-specific neutralizing antibody responses," *Chemistry and Biology*, vol. 10, no. 10, pp. 961–966, 2003.

[17] J. Yang, Y. M. Liu, and Y. Z. Liu, "Advances in the pharmaceutical research on the silymarin," *Natural Product Research and Development*, vol. 16, no. 2, pp. 185–187, 2004.

[18] F. Kvasnička, B. Bíba, R. Ševčík, M. Voldřich, and J. Krátká, "Analysis of the active components of silymarin," *Journal of Chromatography A*, vol. 990, no. 1-2, pp. 239–245, 2003.

[19] C. M. Lin, Y. H. Chen, H. P. Ma et al., "Silibinin inhibits the invasion of IL-6-stimulated colon cancer cells via selective JNK/AP-1/MMP-2 modulation *in vitro*," *Journal of Agricultural and Food Chemistry*, vol. 60, no. 51, pp. 12451–12457, 2012.

[20] R. D. Verschoyle, P. Greaves, K. Patel et al., "Evaluation of the cancer chemopreventive efficacy of silibinin in genetic mouse models of prostate and intestinal carcinogenesis: relationship with silibinin levels," *European Journal of Cancer*, vol. 44, no. 6, pp. 898–906, 2008.

[21] H. J. Cho, D. S. Suh, S. H. Moon et al., "Silibinin inhibits tumor growth through downregulation of extracellular signal-regulated kinase and Akt *in vitro* and *in vivo* in human ovarian cancer cells," *Journal of Agricultural and Food Chemistry*, vol. 61, no. 17, pp. 4089–4096, 2013.

[22] N. Y. Sun, X. L. Wei, B. J. Wu, J. Chen, Y. Lu, and W. Wu, "Enhanced dissolution of silymarin/polyvinylpyrrolidone solid dispersion pellets prepared by a one-step fluid-bed coating technique," *Powder Technology*, vol. 182, no. 1, pp. 72–80, 2008.

[23] M. S. El-Samaligy, N. N. Afifi, and E. A. Mahmoud, "Increasing bioavailability of silymarin using a buccal liposomal delivery system: preparation and experimental design investigation," *International Journal of Pharmaceutics*, vol. 308, no. 1-2, pp. 140–148, 2006.

[24] J. Q. Zhang, J. Liu, X. L. Li, and B. R. Jasti, "Preparation and characterization of solid lipid nanoparticles containing silibinin," *Drug Delivery*, vol. 14, no. 6, pp. 381–387, 2007.

[25] J. N. Yu, Y. Zhu, L. Wang et al., "Enhancement of oral bioavailability of the poorly water-soluble drug silybin by sodium cholate/phospholipid-mixed micelles," *Acta Pharmacologica Sinica*, vol. 31, no. 6, pp. 759–764, 2010.

[26] Y. Wei, X. Ye, X. Shang et al., "Enhanced oral bioavailability of silybin by a supersaturatable self-emulsifying drug delivery system (S-SEDDS)," *Colloids and Surfaces A: Physicochemical and Engineering Aspects*, vol. 396, pp. 22–28, 2012.

[27] Y. Wang, D. Zhang, Z. Liu et al., "*In vitro* and *in vivo* evaluation of silybin nanosuspensions for oral and intravenous delivery," *Nanotechnology*, vol. 21, no. 15, Article ID 155104, 2010.

[28] X. Cao, W. Deng, M. Fu et al., "Seventy-two-hour release formulation of the poorly soluble drug silybin based on porous silica nanoparticles: *in vitro* release kinetics and *in vitro*/*in vivo* correlations in beagle dogs," *European Journal of Pharmaceutical Sciences*, vol. 48, no. 1-2, pp. 64–71, 2013.

[29] I. M. El-Sherbiny, M. Abdel-Mogib, A. A. M. Dawidar, A. Elsayed, and H. D. C. Smyth, "Biodegradable pH-responsive alginate-poly (lactic-co-glycolic acid) nano/micro hydrogel matrices for oral delivery of silymarin," *Carbohydrate Polymers*, vol. 83, no. 3, pp. 1345–1354, 2011.

[30] Z. Chen, D. Pierre, H. He et al., "Adsorption behavior of epirubicin hydrochloride on carboxylated carbon nanotubes," *International Journal of Pharmaceutics*, vol. 405, no. 1-2, pp. 153–161, 2011.

[31] L. Liu, Y. Qin, Z. X. Guo, and D. Zhu, "Reduction of solubilized multi-walled carbon nanotubes," *Carbon*, vol. 41, no. 2, pp. 331–335, 2003.

[32] Y. Ma, W. Z. Li, and J. H. Gu, "Preparation and evaluation of the solid dispersions of poorly soluble silybin," *Journal of Chinese Pharmaceutical Sciences*, vol. 20, no. 6, pp. 604–608, 2011.

[33] S. Sethia and E. Squillante, "Solid dispersion of carbamazepine in PVP K30 by conventional solvent evaporation and supercritical methods," *International Journal of Pharmaceutics*, vol. 272, no. 1-2, pp. 1–10, 2004.

[34] W. Song, Z. Zheng, W. Tang, and X. Wang, "A facile approach to covalently functionalized carbon nanotubes with biocompatible polymer," *Polymer*, vol. 48, no. 13, pp. 3658–3663, 2007.

[35] M. Adeli, F. Hakimpoor, M. Ashiri, R. Kabiri, and M. Bavadi, "Anticancer drug delivery systems based on noncovalent interactions between carbon nanotubes and linear-dendritic copolymers," *Soft Matter*, vol. 7, no. 8, pp. 4062–4070, 2011.

[36] V. Datsyuk, M. Kalyva, K. Papagelis et al., "Chemical oxidation of multiwalled carbon nanotubes," *Carbon*, vol. 46, no. 6, pp. 833–840, 2008.

[37] M. Tang, H. Dou, and K. Sun, "One-step synthesis of dextran-based stable nanoparticles assisted by self-assembly," *Polymer*, vol. 47, no. 2, pp. 728–734, 2006.

[38] S. A. Ntim, O. Sae-Khow, F. A. Witzmann, and S. Mitra, "Effects of polymer wrapping and covalent functionalization on the stability of MWCNT in aqueous dispersions," *Journal of Colloid and Interface Science*, vol. 355, no. 2, pp. 383–388, 2011.

[39] S. Grandi, A. Magistris, P. Mustarelli, E. Quartarone, C. Tomasi, and L. Meda, "Synthesis and characterization of SiO_2-PEG hybrid materials," *Journal of Non-Crystalline Solids*, vol. 352, no. 3, pp. 273–280, 2006.

[40] P. Hou, C. Liu, Y. Tong, S. Xu, M. Liu, and H. Cheng, "Purification of single-walled carbon nanotubes synthesized

by the hydrogen arc-discharge method," *Journal of Materials Research*, vol. 16, no. 9, pp. 2526–2529, 2001.

[41] Y. Li, T. Wang, J. Wang, T. Jiang, G. Cheng, and S. Wang, "Functional and unmodified MWNTs for delivery of the water-insoluble drug Carvedilol—a drug-loading mechanism," *Applied Surface Science*, vol. 257, no. 13, pp. 5663–5670, 2011.

[42] Y. T. Shieh, G. L. Liu, H. H. Wu, and C. C. Lee, "Effects of polarity and pH on the solubility of acid-treated carbon nanotubes in different media," *Carbon*, vol. 45, no. 9, pp. 1880–1890, 2007.

[43] S. H. Hussein-Al-Ali, M. Al-Qubaisi, M. Z. Hussein, M. Ismail, Z. Zainal, and M. N. Hakim, "*In vitro* inhibition of histamine release behavior of cetirizine intercalated into Zn/Al- and Mg/Al-layered double hydroxides," *International Journal of Molecular Sciences*, vol. 13, no. 5, pp. 5899–5916, 2012.

[44] L. Dong, L. Yan, W. G. Hou, and S. J. Liu, "Synthesis and release behavior of composites of camptothecin and layered double hydroxide," *Journal of Solid State Chemistry*, vol. 183, no. 8, pp. 1811–1816, 2010.

[45] Y. S. Ho and A. E. Ofomaja, "Pseudo-second-order model for lead ion sorption from aqueous solutions onto palm kernel fiber," *Journal of Hazardous Materials*, vol. 129, no. 1–3, pp. 137–142, 2006.

[46] R. P. Singh and R. Agarwal, "Prostate cancer prevention by silibinin," *Current Cancer Drug Targets*, vol. 4, no. 1, pp. 1–11, 2004.

[47] B. O. Karim, K. J. Rhee, G. Liu, D. Zheng, and D. L. Huso, "Chemoprevention utility of silibinin and Cdk4 pathway inhibition in $Apc^{-/+}$ mice," *BMC Cancer*, vol. 13, article 157, 2013.